Superplastic Deformation of the 2009-15%SiC_w Composite

R. Kaibyshev[1], V. Kazyhanov[1] and C.C. Bampton[2]

[1] Institute for Metals Superplasticity Problems RAS, Khalturina st., 39, Ufa, 450001, Russia

[2] Rockwell Science Center, 1049 Camino Dos Rios, PO Box 1085, Thousands Oaks, CA 91358, USA

Keywords: Metal Matrix Composite, Superplasticity, Threshold Stress, Grain Boundary Sliding

ABSTRACT

The deformation behavior of the 2009Al - 15%SiC_W reinforced aluminum alloy composite produced via a powder technology method has been studied by tension and compression tests. The effects of modes and conditions of deformation on mechanical properties are considered. The investigation has been performed in the range of strain rates 10^{-5} - 10^{1} s^{-1} at temperatures 450-525°C. Analysis of mechanical behavior showed that the composite displayed features of superplasticity typical for some fine grained conventional aluminum alloys at these temperature-strain rate conditions. The transition from tension to compression results in a shift of the optimal region of superplastic deformation toward higher strain rates and an increase of maximum value of coefficient of strain rate sensitivity *m*. Surface observation has shown that this effect is caused by an increase in homogeneous of grain boundary sliding (GBS). The modes of deformation influence the cooperative nature of grain boundary sliding (CGBS). Spacing between surfaces of CGBS is much less at compression tests. In units of average grain size the spacing constitutes about 1 in compression and from 2 to 3 in tension. The deformation behavior of the composite has been analyzed in terms of threshold stress.

1. INTRODUCTION.

It is known [1] that superplastic deformation is an effective route to increase the hot workability of metal matrix composites (MMCs). Discontinuously reinforced composites exhibit superplastic behavior at relatively high strain rates ($\dot{\varepsilon}$>10^{-2} s^{-1}) [1]. This phenomenon was defined as high strain rate superplasticity (HSRS) [1-4]. Unfortunately, the origin of HSRS in MMCs is not yet clear. Nieh *et al.* [2] suggested a rheological model in which semi-solid is to be regarded as a Newtonian fluid. It was caused by the fact that the phenomenon of HSRS in MMCs was observed at temperatures close to or above the matrix solidus temperature [1-3]. However, the model [4] is in conflict with experimental results. If this model is correct, the coefficient of strain rate sensitivity and elongation-to-failure may not depend on strain rate. To solve this contradiction Mabuchi *et al.* [3, 6] suggested that HSRS of the composites should be caused by relaxation of stress concentrations due to sliding along interfacial boundaries. However, the surface investigation presented in work [3] did not reveal any evidences of interfacial GBS. Most of investigations dealt with mechanical behavior of the composite at hot deformation temperatures but experimental information on structure evolution is very minimal. This severely inhibits a detailed analysis of deformation mechanism.

It is known for monolithic materials that transition from tensile deformation to compression test results in shift of the optimal strain rate interval for superplastic flow toward higher strain rates by one order [5]. Such experimental estimations for MMCs are lacking.

Thus, the objectives of this work are two-fold: first to examine physical mechanisms of flow that occur during HSRS in a MMC; secondly to determine experimental data for the composite

2009Al-15% SiC_W at different modes of plastic deformation and to give a physical explanation of this effect.

2. EXPERIMENTAL MATERIALS AND PROCEDURES.

The composite 2009Al-15% SiC_W was produced via a powder technology method from an aluminum alloy AA2009 (3.8% wt Cu, 1,3% wt Mg, 0.25% wt Si, Al is the balance) and 15% whiskers of SiC in the form of a mill processed 38 mm thick plate.

Tensile samples with the gauge section of 10x5x1.5mm and compression specimens ∅10x13mm were machined from the plate in the longitudinal direction with respect to the original rolling direction. Samples were tested in tension in air at temperatures 450-525^{0}C and at strain rates, from 10^{-5} s^{-1} to 10^0 s^{-1} using a Schenck RMS-100 universal testing machine. A hydraulic testing machine Schenck PSA-100A was used to reach a higher strain rate ($\dot{\varepsilon}=10^0$-10^1 s^{-1}). To evaluate mechanical properties the tensile samples were tested up to failure and compression samples were strained up to ε=50%. The flow stress for each strain rate and for each mode of plastic deformation of the composite was defined as the maximum value of stress. The values of the stress exponent $n=\partial(\lg\dot{\varepsilon})/\partial(\lg\sigma)$ were defined from the slope of the $\lg\varepsilon$-$\lg\sigma$ line. The values of the strain rate sensitivity $m=\partial(\lg\sigma)/\partial(\lg\dot{\varepsilon})$ were calculated as $m=1/n$.

For surface investigation the samples were prepolished by a diamond paste (0.5μm); final polishing was performed using a 20% nitric acid solution in methanol at -30^{0}C and 15 V. Macroscopic scratches on some specimens were used to reveal a type of GBS. The tensile samples were deformed to fixed strains at the strain rate $\dot{\varepsilon}=10^{-2}$ s^{-1} and the compression samples at $\dot{\varepsilon}=10^{-1}$ s^{-1}. Surface examination of deformed specimens was performed using a JSM-840.

3. RESULTS.

3.1 Mechanical properties.

3.1.1 Tension test.

Typical true stress-strain curves for the 2009Al-15% SiC_W composite are shown in Figure 1(a). All the curves exhibit an initial region of strain hardening at ε=5-20% (θ_1=3.88). With decreasing strain rate the initial stage of plastic deformation becomes shorter. In stage 2, the flow stress gradually increases. However the strain hardening coefficient $\theta 2=1.22$ is much less than in stage 1. Stress maximum is reached after the strain ε=30-40%. The peak strain does not significantly depend on strain rate. In stage 3, after the stress peak a gradual stress softening occurs until failure. This may not be true strain softening but is probably a test artefact resulting from localized necking which is included in the stress calculation.

Inspection shows that there is a sigmoidal relationship between the σ and the ε plotted on a double logarithmic scale [5], divided into three distinct regions (Fig.2). Deformation, with high elongation-to-failure occurs over a range of strain rates $\dot{\varepsilon}$=0.01-0.1 s^{-1} at T=500-525^{0}C. The maximum values of the elongation (δ=140%) and the coefficient of strain rate sensitivity m=0.26 are observed at T=525^{0}C and the strain rate $\dot{\varepsilon}$=0.6 s^{-1}. Notably this value of coefficient m is slightly less than 0.3 that is the bottom border for superplasticity. However, there are decreases in the total elongation and the m coefficient values both at lower strain rates in region I and at higher strain rates in region III.

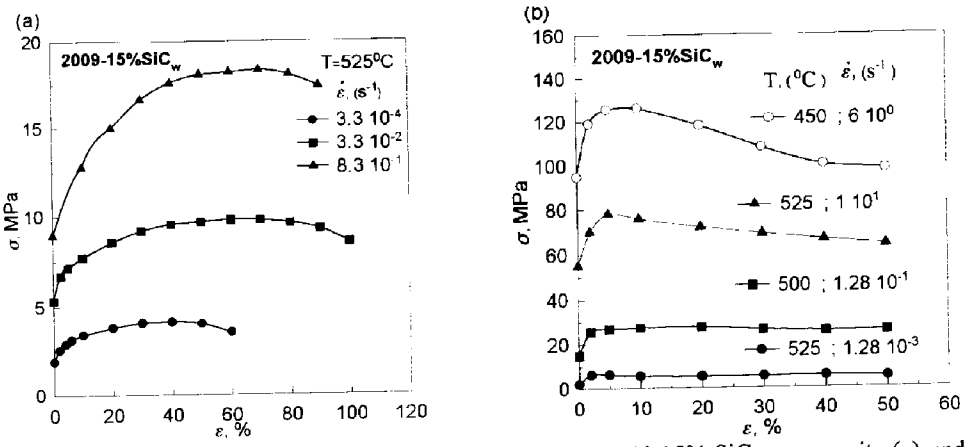

Figure 1. Typical types of stress-strain curves for the 2009Al-15% SiC_W composite;(a) under tension test, (b) under compression test.

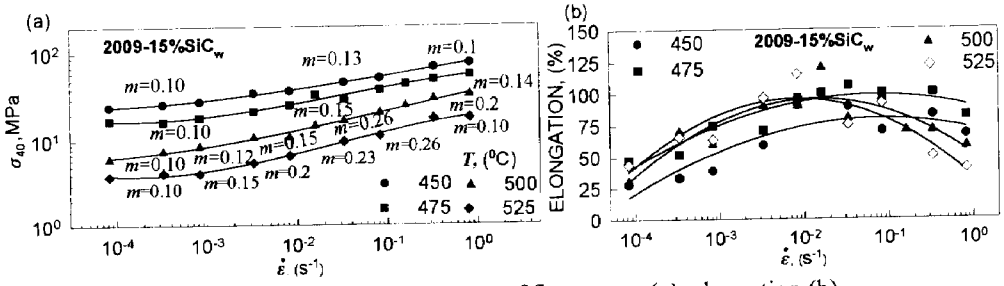

Figure 2. Strain rate dependence of flow stress (a), elongation (b) at various temperatures under tension test.

3.1.2 Compression test.

Typical true stress-strain curves for the composite tested in compression are shown in Figure 1(b). There are two types of the $\sigma-\varepsilon$ curve. At the strain rates ($\dot{\varepsilon}\leq 10^{-2}$ s^{-1}) the stable stage of plastic flow is achieved after small strain ε=2-3%. Another type of the $\sigma-\varepsilon$ curve is observed at higher strain rates. This curve has a peak flow stress. A stable stage of plastic flow is reached after ε=40-50%. A value and extension of the stress peak are mainly determined by the strain rate. The strain rate increase leads to an increase in a relative extent of the stress peak and strain, at which the stable stage of plastic flow is attained. The relative value of the stress peak constitutes 5-30% and the peak strain is ε=3-8%.

The steady-state flow stress variation with the imposed strain rate also gives a sigmoidal three-stage relationship (Fig.3). The σ *vs* $\dot{\varepsilon}$ relationships show that superplastic capability is indicated in the temperature range T=500-525°C in compression. It is seen that the aforementioned transition from the one type of $\sigma-\varepsilon$ curve to another coincides with transition from region I to region II. Transition from tensile deformation to compression results in broadening of the optimum strain rate interval for superplastic flow toward higher strain rates by nearly one order and an increase of maximum value of coefficient of strain rate sensitivity m.

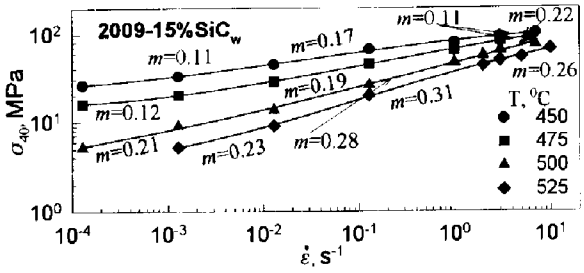

Figure 3. Strain rate dependence of flow stress at various temperatures under compression test.

3.2 Surface microstructural observation.

3.2.1 Tension test.

It has been established that surface metallohraphic features depend on strain and strain rate. Micrographs of the relief evolution in region II are shown in Figure 4. Examination of the specimen surface after deformation revealed direct evidences for CGBS operation [7, 8].

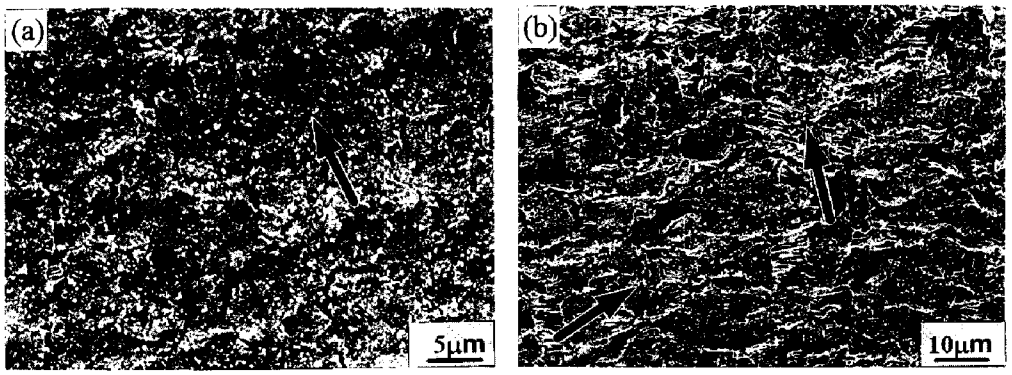

Figure 4. Surface relief after tension deformation at T=525^{0}C initial strain rate of $\dot{\varepsilon}$=8.3·10^{-2} s^{-1}; (a) ε=10%, (b) ε=100%. Note that the tensile axis is horizontal. Arrows indicated directions of the stringers.

After strain ε=10% thin longitudinal deformation bands appear along intergranular boundaries at a distance equal to two units of average initial matrix grain size (Fig. 4a). Observation of these bands is associated with the shifting of matrix grain groups as a unit along common grain boundary surfaces [8]. In macroscale the bands form stringers, which traverse the specimens from one edge to the other. These stringers are discontinuous. In some cases the barriers to band propagation are the SiC whiskers. All the bands tend to align over and are oriented at an angle of 60^o to the tension axis. Transverse bands have not been observed. Further deformation up to strain ε=100% leads to a sharp increase in deformation band broadening (Fig. 4b). At the same time the spacing between surfaces of CGBS remains virtually unchanged. Unlike monolithic alloys [7-11] propagation of deformation bands is retarded by whiskers and becomes discontinuous in manner. The most important feature of the deformation relief after large strain is formation of narrow transverse deformation bands. Their width is less than the width of longitudinal bands by a factor of 5. Connection of secondary transverse bands with primary

longitudinal bands leads to formation of a band network which segments the entire matrix volume. The longitudinal band stringers align at an angle of about 60^{o} to the tension axis.

3.2.2 Compression test.

The transition from tension to compression mode of plastic deformation results in increase of uniformity of CGBS. It is seen (Fig. 5) that the formation of a deformation trace network was observed on the sample surface after strain ε=25%. The length of deformation bands is about 2-8 μm and width is about 0.5-1.5 μm. As a rule, the spacing between GBS surfaces is equal to the average size of matrix grains and constitutes 3-5μm. As compared to samples deformed in tension the spacing between longitudinal and transverse deformation bands is less (Fig. 5a).

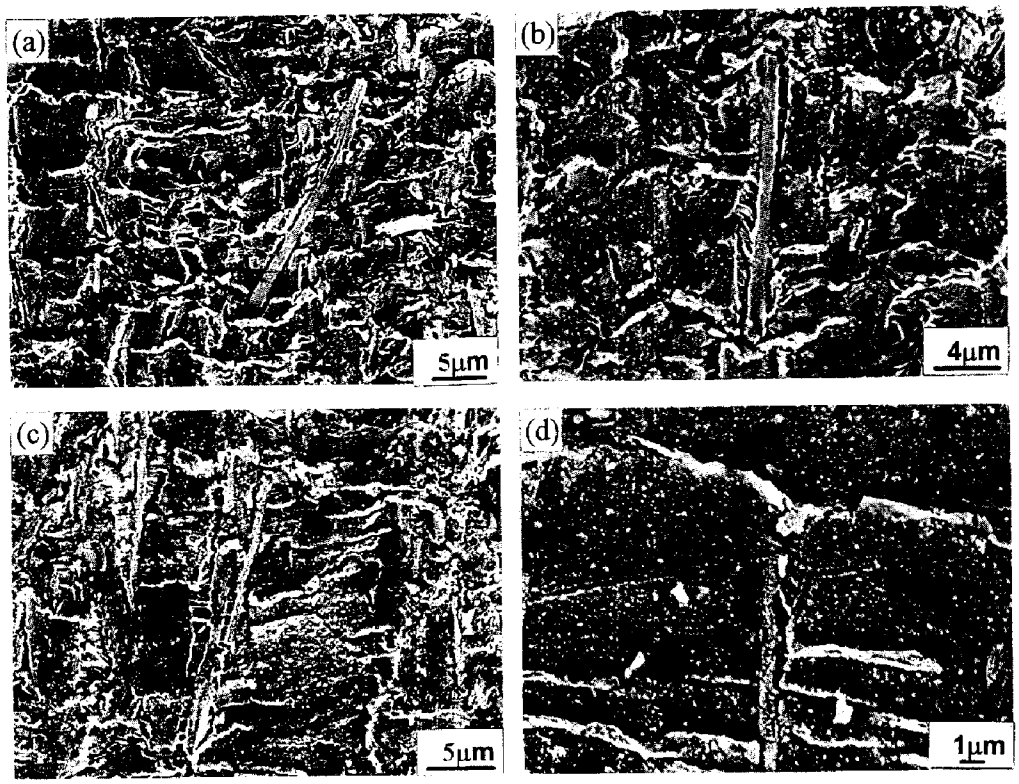

Figure 5. Surface relief after compression deformation at 525^{0}C, $\dot{\varepsilon} = 1.28 \cdot 10^{-1}$ s^{-1}, $\varepsilon = 25\%$. The mutual rotation of grains showing in (a). Strain localization bands along interfacial boundaries in (b) and (c). The shear of scratches along intergranular boundaries in (d) Compression axis is vertical.

Primary deformation bands are oriented at an angle of 30-60^{o} with respect to the compression axis (Fig. 5b). It is known [8-11] that formation of continuous stringers of CGBS is a necessary condition to render a material superplastic. In general, formation of continuous CGBS surfaces occurs as a result of sliding along intergranular boundaries located near the SiC_W (Fig. 5c). Thus, interfacial sliding is not observed while there is evidence of extensive sliding along intergranular boundaries (Fig. 5d). Evidence of GBS is observed in the vicinity of whiskers only in the case

when the SiC_W is located at an Al/Al boundary. As compared to tensile test GBS is observed along the most boundaries of the matrix. In addition it is seen in Fig. 5 that broadening of formed strain localization bands is much less than in samples tested in tension.

4. DISCUSSION

4.1 Deformation behavior.

4.1.1 Threshold stress.

In this work, a low m value of less than 0.1 was observed in the range of low strain rates for both test methods. This might be caused by the threshold stress. The threshold stress (σ_{th}) can be given by extrapolation to zero strain rate of a straight line which the experimental data were plotted as $\dot{\varepsilon}^{1/n}$ against σ on a double linear scale at a single temperature in the whole experimental range 450-525^{0}C (Fig.6) [13].

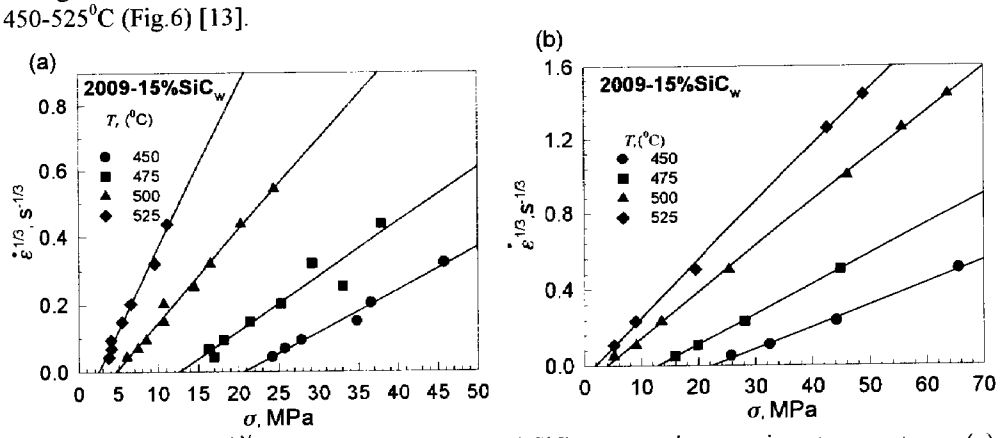

Figure 6. A plot of $\dot{\varepsilon}^{1/n}$ *vs* σ for the 2009Al-15% SiC_W composite at various temperatures: (a) under tension test, (b) under compression test.

Figure 6 represents the plot of $\dot{\varepsilon}^{1/n}$ *vs* σ for n=3. The stress exponent of 3 yields the best linear fit between $\dot{\varepsilon}^{1/n}$ and σ for both test methods. This graphic method can be used if σ_{th} is constant for each test temperature and independent from the strain rate. The prior estimations show that these circumstances apply in regions I and II. The datum points in this strain rate interval most closely fit a straight line whose extrapolation to zero gives the value σ_{th}. It is seen that threshold stress in tension is essentially equal to that in compression.

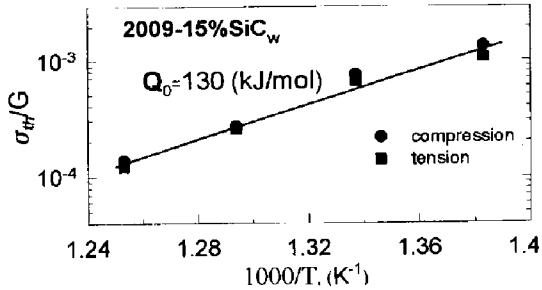

Figure 7. A plot of logarithm of the normalized threshold stress σ_{th}/G *vs* $1/T$.

The temperature dependence of normalized threshold stress σ_{th}/G is presented in Figure 7. It is clear that σ_{th} decreases directly with increasing temperature. This temperature dependence obeys the equation [14]:

$$\sigma_{th}/G=B_O\cdot\exp(Q_O/RT) \quad (1)$$

where B_O is a constant, and Q_O is an energy term. The value Q_O = 130±10 KJ/mol was obtained graphically by plotting $\ln\sigma_{th}/G$ *vs* 1/T for both test methods.

4.1.2. Activation energy.

The true activation energy of deformation Q_C, was determined according to the following equation:

$$Q_c=-R\cdot\left.\frac{\partial(\ln\dot{\varepsilon})}{\partial(1/T)}\right|_{\sigma-\sigma th} \quad (2)$$

True activation energy in the moderate effective stress region (σ_{eff} = 5-30 MPa) of the composite tested in tension is equal to Q=240± 10 kJ/mol and in compression is equal to Q= to 164 ± 6 kJ/mol. The latter value is close to that for the activation energy for lattice self-diffusion (142 kJ/mol).

4.2 Operating deformation mechanisms.

It was shown in the prior work [12] that no segregation or liquid phase formation on interfacial boundaries was observed at the testing temperature 525^{0}C. The analysis of deformation behavior supports this conclusion. It is obvious that the rate-controlling deformation process in the 2009Al - 15%SiC_w composite is associated with deformation in the aluminum matrix. Consequently, this implies that the role of liquid phase is not important for the origin of HSRS in the composite at this temperature. The consistent feature of presented experiments of surface microstructural observation is that sliding along intergranular boundaries is the dominant flow mechanism. This mechanism of plastic deformation is responsible for features of deformation behavior of the composite tested in tension and compression. The occurrence of extensive CGBS is evident from direct surface microstructural observation and consistent with the experimental values of $m\geq0.3$ in compression [3, 5]. There are strong grounds to believe that the contribution from GBS in aluminum matrix to the total elongation is as high as in monolithic aluminum alloys (about 50%-70% in region II) [5].

4.3 The effect of deformation mode on superplasticity of the composite.

It is known [11], that in two-phase materials CGBS occurs due to the movement of extrinsic cellular dislocation through switching of neighbors by sliding grains. This causes mutual sliding of grain groups as undeforming units. The size of grain groups affects the optimal strain rate of superplasticity, the total elongation and the maximum value of the strain rate sensitivity parameter m [8, 11]. In previous work [8] the following relationship between the total strain rate ($\dot{\varepsilon}$) and the strain rate due to GBS ($\dot{\varepsilon}_{GBS}$) was proposed:

$$\dot{\varepsilon}=\dot{\varepsilon}_{GBS}/s \quad (3)$$

where s is the spacing of CGBS surfaces in units of average grain size. It was observed in numerous investigations [7-11] that in single-phase monolithic alloys s ≈5 to 8 at a small strain

and s≈2 to 5 at a high strain. In addition, the grain groups have a right-angle shape. Inspection of literature [7-11] shows that a character of CGBS in the composite is typical for two-phase materials. There are three main feature of CGBS operation in MMCs.
(i) The spacing between GBS surfaces depends slightly on strain.
(ii) In the composite the spacing between surfaces of CGBS is much less than in monolithic alloys.
(iii) The grain groups are equiaxed.
Introduction of SiC reinforcements results in transition of a band shape of the grain groups to a globular shape. This is due to non-homogeneous distribution of the SiC_W in the aluminum matrix. Clusters of whiskers act as barriers for propagation of primary sliding along the plate surfaces of intergranular boundaries. This encourages the activation of a secondary CGBS system and provides the great uniformity of plastic deformation. As a result, the region II of superplasticity in MMCs shifts toward higher strain rates. Thus, the features of CGBS in the composite are dominant factors determining the advent of HSRS in MMCs at pre-melting temperatures.

The influence of the test method on superplastic behavior of the composite is associated with the uniformity of CGBS. In the case of tensile deformation the s value is larger than in compression by a factor of 2. That is why the transition from tension to compression results in a broadening of the optimal region of superplastic deformation toward higher strain rates and *m* coefficient increase.

5. CONCLUSIONS.

The composite 2009Al-15% SiC_W exhibits superplastic behavior at T=500-525°C at strain rates $\dot{\varepsilon}$=0.01-0.1 s^{-1} in tension and at $\dot{\varepsilon}$=0.01-2 s^{-1} in compression. The deformation of the composite is controlled by deformation in the aluminum matrix. The high strain rate of superplastic deformation is caused by greater uniformity of CGBS compared with monolithic alloys. The effect of deformation modes on superplasticity of the composite is also connected with homogeneity of CGBS.

6. REFERENCES

[1]. T. G. Nieh and J. Wadsworth, Mat. Sci. and Eng. **A147,** 129 (1991).
[2] T. G. Nieh, J. Wadsworth and T. Imai, Scr. Metall. Mater. **26,** 703 (1992).
[3] M. Mabuchi, K. Higashi and T. G. Langdon, Acta Metall. Mater. **42,** (5), 1739 (1994).
[4] R. S. Mishra, T. R. Bieler and A. K Mukherjee, Acta. Metall. Mater. **43,** 893 (1995).
[5] O. A. Kaibyshev , Superplasticity of Alloys, Intermetallides, and Ceramics (Berlin, Springer-Verlag,), .316 (1992).
[6] M. Mabuchi and K. Higashi, Phil. Mag. Let. **70,** 1 (1994).
[7] V. V. Astanin, O. A. Kaibyshev and S. N. Faizova, Acta Met. Mat. **42,** 2617 (1994).
[8] M. G. Zelin, N. A. Krasilnikov, R. Z. Valiev, M. W. Grabski, H. S. Yang and A. K. Mukherjee, Acta Metall.Mater. **42,** 119 (1994).
[9] M. G. Zelin and A. K. Mukherjee, Phil. Mag. **68,** 1183 (1993).
[10] V. V. Astanin, The Physics of Metals and Metallograthy **79,** 166 (1995). (*in Russian*).
[11] M. G. Zelin and A. K. Mukherjee, Acta Metall. Mater.**43,** 2359 (1995).
[12] R. S. Mishra, C. Echer, C. C. Bampton, T. R. Bieler and A. K. Mukherjee, (in the press)
[13] F. A. Mohamed., K. T. Park and E. J. Lavernia, Mat. Sci. and Eng. **A150,** 21 (1992).
[14] K. T. Park, E. Lavernia and F. Mohamed, Acta Metall. Mater. **42,** 667 (1994).